Inaba Y, et al.	undergoing chemotherapy with first-line FOLFOX.				
Inaba Y, Arai Y, Aramaki T, et al.	IPhase I/II Study of Hepatic Arterial Infusion Chemotherapy With Gemcitabine in Patients With Unresectable Intrahepatic Cholangiocarcinoma (JIVROSG-0301).	Am J Clin Oncol	[Epub ahead of print] 2010		2010
Sakaino S, Takizawa K, Nakajima Y, et al.	Percutaneous vertebroplasty performed by the isocenter puncture method.	Radiat Med	26	70-75	2008
香田渉，小林健，南哲也，高仲強，山田圭輔，武川治水，松井修	骨腫瘍に対する経皮的椎体形成術の現況と最前線	映像情報メディカル	41	608-612	2009
曽根美雪,江原茂，荒井保明，小林健	IVRのエビデンスを創るための研究デザイン	断層映像研究会雑誌	36	96-104	2009
大須賀慶悟、穴井洋、高橋正秀、宮山士朗、山上卓士、曽根美雪、中村仁信	肝動脈塞栓剤・多孔性ゼラチン粒（ジェルパート）のマイクロカテーテル通過前後の粒子径と断片化に関する検討.	癌と化学療法	36(3)	437-442	2009
曽根美雪、江原茂	Refresher Course: IVR医のための臨床研究の基本	画像診断	29(5)	532-539	2009
曽根美雪、中島康雄、塩山靖和、鶴崎正勝、平木隆夫、金沢　右、吉松美佐子、加山英夫、柿田聡子、ウッドハムス玲子、西巻　博、興梠征典、後藤靖雄、成松芳明	産科出血に対するIVR：日本IVR学会ガイドライン委員会の取り組み	IVR会誌	24	138-141	2009
曽根美雪、江原茂、荒井保明、小林健	EBMの実践と画像診断. IVR研究のストラテジー	断層映像研究会誌	36(2)	96-104	2009
渡辺裕一，岡田守人，楫靖，里内美弥子，佐藤洋造，山邉裕一郎，女屋博昭，遠藤正浩，曽根美雪，荒井保明	固形がんの新効果判定規準　改訂RECISTガイドライン(version 1.1)	癌と化学療法	36(13)	2495-501	2009
Matsumoto K, Inaba Y, et al	Ruptured pseudoaneurysm of the splenic artery complicating endoscopic ultrasound-guided fine-needle aspiration biopsy for pancreatic cancer.	Endoscopy.	42	E27-E28	2010
山浦秀和、稲葉吉隆、他	集学的治療における肝動注化学療法の位置づけ	外科	72	153-157	2010
Kanemitsu Y, Inaba Y, et al	A randomized phase II/III trial comparing hepatectomy followed by mFOLFOX6 with hepatectomy alone as treatment for liver metastasis from colorectal cancer: Japan Clinical Oncology Group Study JCOG0603. Col	Jpn J Clin Oncol.	39	406-409	2009

	orectal Cancer Study Group (CCSG) of Japan Clinical Oncology Group.				
名嶋弥菜、稲葉吉隆、他	肝動脈化学塞栓療法のエビデンス	腫瘍内科	4	307-312	2009

IV. 研究成果の刊行物・別刷

INTERNAL MEDICINE

□ CASE REPORT □

Jejunogastric Intussusception: Life-Threatening Complication Occuring 55 Years after Gastrojejunostomy

Hiroyuki Tokue[1], Yoshito Tsushima[2], Yasuaki Arai[1] and Keigo Endo[2]

Abstract

An 80-year-old man presented with acute abdominal pain and hematemesis. He had a history of gastrojejunostomy 55 years previously. Ultrasonography (US) showed intragastric tublar images with peristalsis. Enhanced computed tomography (CT) demonstrated a dilated stomach with an intragastric filling by bowel loops suggestive of jejunogastric intussusception (JGI). Reduction of the JGI was immediately performed without resection of the intussuscepted intestine, and the patient was well postoperatively.

JGI is a rare life-threatening complication after gastric surgery. This complication may occur even 55 years after gastric surgery, and preoperative diagnosis is possible by US and CT findings.

Key words: jejunogastric intussusception, invagination, gastric surgery, computed tomography, ultrasonography

(Inter Med 48: 1657-1660, 2009)
(DOI: 10.2169/internalmedicine.48.2115)

Introduction

Jejunogastric intussusception (JGI) is a rare life-threatening complication of gastrectomy or gastrojejunostomy. It usually occurs with abdominal pain, nausea, vomiting, and hematemesis. Diagnosis of this condition has been reported to be difficult in most of the cases, although a history of gastric surgery can help in making a diagnosis. An early diagnosis and urgent surgical intervention are essential. We present a case of the characteristic US and CT findings of this entity.

Case Report

An 80-year-old man presented with acute abdominal pain and hematemesis. He had undergone gastrojejunostomy (Billroth II reconstruction) for a bleeding duodenal ulcer 55 years previously. Physical examinations disclosed epigastric tenderness and a soft non-distended abdomen. His vital signs were normal and blood counts and laboratory examinations were unremarkable. Ultrasonography (US) showed intragastric tublar images with peristalsis (Fig. 1), and enhanced computed tomography (CT) demonstrated a dilated stomach with an intragastric filling by bowel loops (Fig. 2). We suspected JGI based on imaging findings, and endoscopy confirmed it with petechial hemorrhage (Fig. 3). Emergent surgery revealed a severely dilated stomach stump and a 40 cm-long efferent intestinal loop which had intussuscepted in a retrograde direction into the remnant gastric lumen, passing over the Braun's anastomosis (Fig. 4). His operative findings were Billroth II retrocolic loop gastrojejunostomy. The efferent loop was edematous with serosal petechiae but absolutely viable. No abnormalities such as a tumor, ulcer, diverticulum, or stenosis were identified that could have acted as a point for the intussusception. Reduction of the JGI was performed by Hutchinson's procedure without resection of the intussuscepted intestine. He was well postoperatively and discharged nine days after operation. On follow-up, his postoperative course was uneventful.

Discussion

JGI was first described by Bozzi (1) in a patient after gastrojejunostomy, and it was also reported in patients after Billroth I reconstruction, Billroth II reconstruction, total gas-

[1]Division of Diagnostic Radiology, National Cancer Center Hospital, Tokyo and [2]Department of Diagnostic and Interventional Radiology, Gunma University Hospital, Maebashi
Received for publication February 3, 2009; Accepted for publication May 27, 2009
Correspondence to Dr. Hiroyuki Tokue, tokue@s2.dion.ne.jp

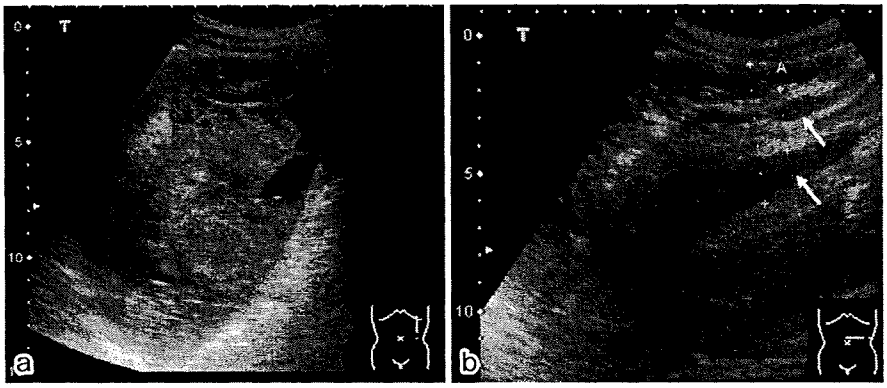

Figure 1. **A 80-year-old man presented with abdominal pain and hematemesis. (a) Sagittal US demonstrated intragastric tubular images with peristalsis. (b) Transverse US revealed a sandwich-like appearance (arrows) of the alternating loops of bowel with a loop-within-loop appearance.**

Figure 2. **(a) Enhanced CT showed a distended stomach with an intragastric filling by bowel loops (arrow). (b) Mesenteric fat and vessels were followed into the intussusception with central area of fat density and vessels (arrow).**

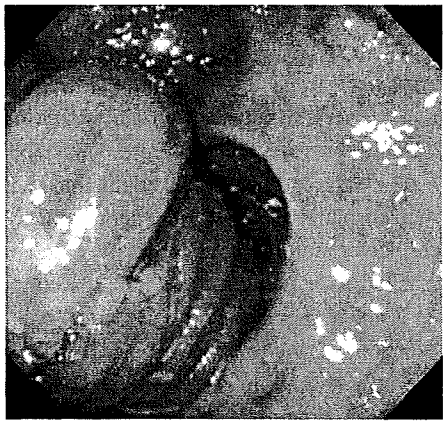

Figure 3. **Gastric endoscopy showed a lobulated congestive mass which was consistant with jejunogastric intussusception.**

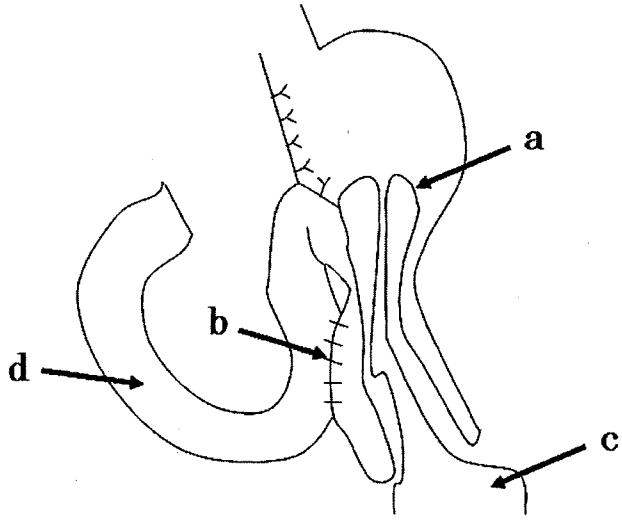

Figure 4. **The operative findings: (a) retrograde jejunogastric intussusception (b) Braun's anastomosis (c) dilated efferent loop (d) afferent loop.**

trectomy, Roux-en-Y gastric bypass, and a pancreaticojejunostomy (2-4). The incidence of JGI has been estimated to be three in 2000 gastrojejunostomies (0.15%) (5). Although there have been many cases reports about JGI in the surgical literature (6-8), it has been rarely reported in the field of internal medicine. A possible race difference has not been investigated, however, the incidence may be extremely low in Asia; there have only been a few case reports from Asian countries (9, 10). Physician should be aware of the US and CT findings of this life-threatening complication after gastric

surgery.

The etiology of JGI is unclear. Two major theories are functional and mechanical. The most widely accepted functional theory is the disordered motility with functional hyperperistalsis triggered by spasm or hyperacidity (11). Mechanical factors include adhesions, a long mesentery, gastric derangements, and a sudden increase in abdominal pressure (12). An acute and a chronic form of JGI have been clinically recognized (5). Incarceration and strangulation of the intussuscepted loop generally occur in the acute form. On the other hand, spontaneous reduction is typical in the chronic type. Thus, the acute form like the present case is characterized by acute severe colicky epigastric pain, vomiting and, subsequently, hematemesis. JGI is classified into three anatomic types according to the invaginated loop (13), type I: afferent loop invagination, type II: efferent loop invagination, type III: the intussusception of both. A type II invagination is observed in 80% of cases (3) and our case was classified type II.

Shiffman and Rappaport (6) emphasized that loose mucosa at the anatomotic site may prolapse into the gastric pouch during normal peristalsis. This could explain the less common afferent loop intussusception. Karlstrom and Kelly (14) suggested that ectopic pacemakers present in the Roux limb after vagotomy and Roux gastrectomy drive the limb in the reverse direction and slow emptying of liquids after operation. The defect can be corrected by pacing the Roux limb in the forward direction. In the present case, the efferent loop was found intussuscepted in a retrograde way into the gastric lumen. These reports may explain the cause of the present case. JGI has occurred between five days to 35 years after surgery (5). The present case occurred 55 years after surgery and as far as we know this case is the longest period from operation in past reports.

US is the method of first choice because it can be performed at bedside without ionizing radiation and is cost-effective. CT allows the differentiation of the distinct stages of the disease and the views given by CT are often more easily accepted by the surgeons. It is important to understand the typical imaging findings of JGI. In most cases, US shows intragastric tubular images with peristalsis and CT shows a dilated stomach with intragastric filling by bowel loops (3, 15). Most reported cases of JGI were diagnosed at surgery (16), but we suspected that the typical findings enable us to make preoperative diagnosis. Although spontaneous reduction was reported, in most cases surgical management should be performed as soon as possible to avoid the additional risk of severe complications. Surgical options include reduction, resection of the compromised bowel, revision of the anastomosis, and the takedown of the anastomosis, depending on the conditions found during the operation (3). When there is ischemic change of the invaginated loop, resection is the only treatment option. In the acute setting, the morbidity and mortality figures vary considerably, with mortality rates rising significantly from 10 to 50% with 48 hours delay in surgical correction (17). The fixation of the jejunum to the adjacent tissue, mesocolon, colon, or stomach may obviate the recurrence (18).

Conclusion

JGI is a rare life-threatening complication of gastric surgery which is often diagnosed at surgery. There is a wide variation in the lapse time between the gastric surgery and the occurrence of JGI. This complication may occur even 55 years after gastric surgery; preoperative diagnosis is possible by US and CT findings. We should be aware of these imaging findings to avoid mortality.

References

1. Bozzi E. Annotation. Bull Acad Med **122**: 3-4, 1914.
2. Lundberg S. Retrograde dunndarminvagination nach gastroenterostomie. Acta Chir Scand **54**: 423-433, 1922.
3. Archimandritis AJ, Hatzopoulos N, Hatzinikolaou P, et al. Jejunogastric intussusception presented with hematemesis: a case presentation and review of the literature. Gastroenterol **1**: 1, 2001.
4. Goverman J, Greenwald M, Gellman L, Gadaleta D. Antiperistaltic (retrograde) intussusception after Roux-en-Y gastric bypass. J Am Coll Surg **199**: 988-989, 2004.
5. Marx WJ. Reduction of jejunogastric intussusception during upper gastrointestinal examination. Am J Roentgenol **131**: 334-335, 1978.
6. Shiffman M, Rappaport I. Intussusception following gastric resection. Am Surg **32**: 715-724, 1966.
7. Salem MH, Coffman SE, Postlethwait RW. Retrograde intussusception at the gastrojejunal stoma. Ann Surg **150**: 864-871, 1959.
8. Wheatley MJ. Jejunogastric intussusception diagnosis and management. J Clin Gastroenterol **11**: 452-454, 1989.
9. Hashimoto Y, Akagi S, Sakashita Y, et al. Usefulness of computed tomography as a preoperative diagnostic modality in a case with acute jejunogastric intussusception. J Gastrointest Surg **11**: 1078-1080, 2007.
10. Su MY, Lien JM, Lee CS, Lin DY, Tsai MH. Acute jejunogastric Intussusception: report of five cases. Chang Gung Med J **24**: 50-56, 2001.
11. Robertson DS, Weder C. Acute jejunogastric intussusception. Can J Surg **1**: 210-214, 1968.
12. Bundrick TJ, Turner MA, Cho SR. Retrograde jejunogastric intussusception. Rev Interam Radiol **6**: 21-24, 1981.
13. Shackman R. Jejunogastric intussusception. Br J Surg **27**: 475-480, 1940.
14. Karlstrom L, Kelly KA. Ectopic jejunal pacemakers and gastric emptying after Roux gastrectomy: effect of intestinal pacing. Surgery **106**: 867-871, 1989.
15. Navid AZ, Stephanie PH, Mark RR. Jejunogastric intussusception: a case report with the review of literature. Emerg Radiol **13**: 265-267, 2007.
16. Mele CD, Porayko K. Jejunogastric intussusception, an indication for emergent endoscopy: case report. Gastrointest Endosc **57**: 593-595, 2003.
17. Achyut JM, Ishwar JM, Jayantkumar BD, et al. Jejunogastric intussusception: case report and review of the literature. Dig Endosc **16**: 88-90, 2004.
18. Lopez-Mut JV, Cubells M, Campos S, Miranda V, Rivera P. Je-

junogastric intussusception: a rare complication of gastric surgery. Abdom Imaging **23**: 558-559, 1998.

Ann Nucl Med (2009) 23:235–243
DOI 10.1007/s12149-009-0230-z

ORIGINAL ARTICLE

Role of carbon-11 choline PET/CT in the management of uterine carcinoma: initial experience

Keitaro Sofue · Ukihide Tateishi · Morio Sawada · Tetsuo Maeda · Takashi Terauchi · Daisuke Kano · Yasuaki Arai · Tomio Inoue · Kazuro Sugimura

Received: 12 September 2008 / Accepted: 27 November 2008 / Published online: 31 March 2009

Abstract
Purpose The present study was conducted to clarify the role of carbon-11 choline (^{11}C-choline) positron emission tomography (PET)/computed tomography (CT) in the management of uterine carcinoma.
Materials and methods Twenty-two patients who underwent ^{11}C-choline PET/CT and pelvic MRI were evaluated retrospectively. The images were reviewed by a board-certified radiologist and a nuclear medicine specialist who were unaware of any clinical information, and a consensus was reached. Diagnostic accuracy of PET/CT was evaluated for staging. The reference standard consisted of histological examination ($n = 17$) and follow-up conventional CT ($n = 5$). In five patients with cervical carcinoma, ^{11}C-choline PET/CT was performed before and after treatment that consisted of cisplatin infusion and subsequent radiotherapy. Standardized uptake value (SUV) was compared with unidimensional and volumetric measurements that were made on magnetic resonance images (MRI) before and after treatment.
Results Based on PET/CT interpretations, the reviewers correctly classified T stage in 8 patients (47%), N stage in 21 patients (96%), M stage in 20 patients (91%), and TNM stage in 15 patients (88%). Tumor size, volume, and SUV decreased after treatment in five patients with cervical carcinoma. Using the Pearson correlation test, a significant correlation was found between the reduction rate of SUV and reduction rate of tumor volume.
Conclusions ^{11}C-choline PET/CT is an accurate means for the management of patients with uterine carcinoma. The combination of ^{11}C-choline PET/CT and MRI increases the accuracy of staging in patients with uterine carcinoma.

Keywords PET/CT · Choline · Uterine

K. Sofue · Y. Arai
Division of Diagnostic Radiology,
National Cancer Center Hospital, Tokyo, Japan

U. Tateishi (✉) · T. Inoue
Department of Radiology, Yokohama City University
Graduate School of Medicine, 3-9 Fukuura, Kanazawa-ku,
Yokohama, Kanagawa 236-0004, Japan
e-mail: utateish@yokohama-cu.ac.jp

M. Sawada
Division of Gynecologic Oncology,
National Cancer Center Hospital, Tokyo, Japan

T. Maeda · K. Sugimura
Department of Radiology, Kobe University Graduate
School of Medicine, Hyogo, Japan

T. Terauchi · D. Kano
Division of Cancer Screening,
Research Center for Cancer Prevention and Screening,
National Cancer Center, Tokyo, Japan

Introduction

Positron emission tomography (PET) with carbon-11 choline (^{11}C-choline) has been used to evaluate patients with a variety of malignant tumors [1–7]. Most studies have revealed that ^{11}C-choline PET is useful in the assessment of tumor stage [3–7]. More recently, PET studies using ^{11}C-choline as a tracer have been reported in patients with prostate cancer because of the minimal background activity in the pelvis due to the low level of excretion via the urinary tract which interferes with image evaluation [8]. ^{11}C-choline PET is also a feasible means of imaging uterine carcinomas [9], but the role of ^{11}C-choline PET scans in the preoperative staging of uterine carcinoma has not been clarified.

In the response evaluation criteria in solid tumors (RECIST), CT and magnetic resonance imaging (MRI) are considered the best currently available and the most useful tools for assessing the therapeutic effect on the target lesions, and the maximum diameter for the target lesions used as the reference to the objective tumor response [10]. However, the limited value of the RECIST criteria has been pointed out. PET with [^{18}F]-fluoro-2-deoxy-glucose (18F-FDG) has been used in the evaluation of patients with solid tumors, because the metabolic reduction precedes morphological changes [11]. Most studies on therapeutic response reveal that 18F-FDG-PET is superior in the assessment of therapeutic monitoring compared with conventional imaging [12–15]. PET has the potential to therapy monitoring in patients with cervical carcinoma. However, the exact role of ^{11}C-choline PET scan in the assessment of tumor response for cervical carcinomas has not been elucidated fully.

Positron emission tomography/computed tomography can improve tumor localization and staging accuracy because the anatomic and molecular information can be precisely co-registered [16]. The aim of the current study was to clarify the exact role of ^{11}C-choline PET/CT in the management of uterine carcinoma.

Materials and methods

Patients

We retrospectively reviewed the results of ^{11}C-choline PET/CT from January 2006 to December 2006 in patients with uterine carcinoma who either underwent radical hysterectomy and pelvic lymphadenectomy or were started on chemotherapy within a week. ^{11}C-choline PET/CT had been performed only for patients who had provided written informed consent to participate in the study and to a review of their records and images. A total of 22 patients with uterine carcinoma (cervical carcinoma, $n = 11$; corpus carcinoma, $n = 11$), which included preoperative studies for initial staging in all 22 patients, were enrolled into this study. In five patients with cervical carcinoma, both initial and follow-up examinations after chemotherapy in five patients were performed. The mean age was 51 years (range 31–73 years). The clinical records of all 22 patients were available for review. This study was conducted in accordance with the amended Helsinki declaration, and the protocol was approved by the Institutional Review Board.

PET/CT

Studies were performed with the LSO-based whole-body PET/CT scanner (Aquiduo;Toshiba). The CT component of the scanner was the same as that of Aquillion 16, which has 16-rows detector. The PET component of the scanner has a transaxial field of view of 68.3 cm and an axial field of view of 16.2 cm without septa and rotating rod source. The scanner was used in 3D mode with image resolution of 4.0 mm in full width at half maximum (FWHM). Prior to the ^{11}C-choline PET/CT study, the patients fasted for at least 6 h. CT was performed from the head to the mid-thigh according to a standardized protocol with the following settings: axial 2.0-mm collimation × 16 modes; 120 kVp; Auto-Exposure Control (SD10); and a 0.5-s tube rotation, a table speed of 11.0 mm/s. Patients maintained normal shallow respiration during the acquisition of CT scans. No iodinated contrast material was administered. ^{11}C-choline was synthesized with a commercial module described by Hara and co-workers [17]. Acquisition of emission scans from the head to the mid-thigh was started 5 min after intravenous administration of a mean ^{11}C-choline dose of 464 MBq (range, 409-560 MBq). Second emission scans of the pelvis were subsequently obtained starting 17 min of uptake time. The acquisition time for PET was 2 min per table position. Images were reconstructed with attenuation-corrected ordered-subset expectation maximization with 4 iterations and 14 subsets using emission scans and CT data.

Magnetic resonance imaging

MRI was performed within 2 weeks of ^{11}C-choline PET/CT, both before and after treatment. MRI was performed using a 1.5 T system (Signa Horizon LX, GE Medical Systems, Milwaukee). Pulse sequences comprised T1-weighted spin echo (SE) images (TR (repetition time)/TE (echo time): 500–600 ms/7–10 ms), T2-weighted fast spin echo (FSE) images (TR/TE: 3,750–4,400 ms/98–105 ms), as well as post-contrast T1-weighted SE images (TR/TE: 580–645 ms/6–10 ms) with fat suppression after injection of contrast material. All images were acquired in the transverse plane with a slice thickness of 5.0 mm, and a 1.0 mm intersection gap. The contrast material used was gadopentetate dimeglumine (Magnevist, Bayer Schering Pharma, Osaka, Japan) at a dose of 0.1 mmol/kg body weight. Pulse sequence parameters and slice orientation varied with the examined anatomic site. The images were reviewed and a consensus was reached by two board-certified radiologists who were unaware of any clinical or radiological information using multimodality computer platform.

Image interpretation

The images were reviewed by a board-certified radiologist and a nuclear medicine specialist who were unaware of any clinical information and a consensus was reached. PET,

CT, MRI, and co-registered PET/CT images were analyzed with dedicated software (e-soft; Siemens). PET, CT, and MRI were interpreted separately and co-registered PET/CT was read 6 months after the initial review. ^{11}C-choline uptake was considered abnormal when substantially greater than that of the surrounding normal tissue. A region of interest (ROI) of 1 × 1–3 × 3 pixels was manually outlined within regions of increased ^{11}C-choline uptake and measured on each slice. For quantitative interpretations, the standardized uptake value (SUV) was determined according to the standard formula, with activity in the ROI recorded as Bq per ml/injected dose in Bq per weight (kg), but time decay correction for whole-body image acquisition was not performed. The maximum SUV (SUV max) was recorded using the maximum pixel activity within the ROI. We obtained 40% of maximum counts as the activity threshold. Both SUV max at a mean uptake time of 5 and 17 min were recorded as SUV_1 and SUV_2, respectively. The change in SUV was also calculated according to the formula: δ SUV (%) = $(SUV_1 - SUV_2)/SUV_1 \times 100$. Uni-dimensional and volumetric measurements were conducted on MRI by the single radiologist. On the uni-dimensional measurement, tumor size was defined as the maximum diameter. On the volumetric measurement, tumor volume was calculated by a slice-by-slice evaluation. The area of the tumor was manually measured slice-by-slice on the transaxial post-contrast T1-weighted SE images with fat suppression, using manual segmentation with the multimodality computer platform. The measured area (cm^2) per slice was multiplied by the factor 0.6 cm. The factor of 0.6 cm is based on the slice thickness of 5 mm and a distance factor of 1 mm. The volume of all measured slices containing tumor was summed up for total tumor volume.

Staging in cervical carcinoma

Tumor size by ^{11}C-choline PET/CT was determined based on the CT portion of the PET/CT. In tumors with unclear contour, tumor size was determined as the diameter of the cervix. T1 was considered when localized tumor with ^{11}C-choline uptake was depicted in the cervix. T2 was considered when tumor invaded the parametrium with ^{11}C-choline uptake for cervical carcinoma. T3 was considered when tumor with ^{11}C-choline uptake involved the serosa, adnexa, vagina, or peritoneal dissemination. Lymph nodes with abnormal uptake were recorded as positive for metastasis even when their short-axis diameter was less than 10 mm. N stage in six patients was confirmed by pathologic examination of specimens obtained by sampling of regional nodes. Nodal status of extraregional lymph nodes was confirmed in five patients by obvious regression in size of the lesions on follow-up MR examinations after treatment. M stage was determined when paraaortic lymph node was involved or distant metastasis was found on contrast-enhanced CT during follow-up.

Staging in corpus carcinoma

Tumor size was also determined based on the CT portion of the PET/CT. In tumors with unclear contour, tumor size was determined as the diameter of the corpus. T1 was considered when localized tumor with ^{11}C-choline uptake was depicted in the corpus. T2 was considered when tumor involved the cervix with ^{11}C-choline uptake. T3 was considered when tumor with ^{11}C-choline uptake involved the serosa, adnexa, vagina, or peritoneal dissemination. Lymph nodes were classified similarly to those of cervical carcinoma. N stage was confirmed by pathologic examination of specimens obtained by sampling of regional nodes in all patients. M stage was determined when distant metastasis was found on contrast-enhanced CT during follow-up.

Treatment

In five patients with cervical carcinoma, treatment consisted of cisplatin infusion and subsequent radiotherapy. All but one of the patients, except one, were received chemotherapy consisting of cisplatin. One patient who had renal dysfunction did not receive chemotherapy. Radiotherapy comprised external beam radiotherapy (EBRT) 50 Gy and intra-cavitary radiotherapy (ICRT) 18–24 Gy. EBRT of the whole pelvis was performed and a total dose of 50 Gy was delivered at the rate of 2 Gy per fraction in 5 weeks. ICRT was performed and a total dose of 18–24 Gy was delivered at the rate of 8 Gy per fraction once a week. Four patients underwent chemotherapy with cisplatin (range 56–63 mg; mean 60.3 mg) once a week during EBRT. ^{11}C-choline PET/CT scans were performed before the start of treatment and after treatment.

Assessment of therapeutic response

The tumor size and volume from MRI after treatment were compared with those from the baseline study. The percentage of size reduction rate (%Size-RR) was calculated by the following formula; [Size (baseline) − Size (after treatment)]/Size (baseline) × 100 (%). The percentage of volume reduction rate (%Volume-RR) was calculated by the following formula; [Volume (baseline) − Volume (after treatment)]/Volume (baseline) × 100 (%).

Evaluation of metabolic response was accomplished by comparing the relative change in SUV, the percentage of SUV reduction rate (%SUV-RR). The SUV_1 and the SUV_2 from ^{11}C-choline PET/CT after treatment were compared with the baseline study. The percentage SUV_1 reduction

rate (%SUV_1-RR) was defined as the following formula; [SUV_1 (baseline) − SUV_1 (after treatment)]/SUV_1 (baseline) × 100 (%). The percentage SUV_2 reduction rate (%SUV_2-RR) was defined as the following formula; [SUV_2 (baseline) − SUV_2 (after treatment)]/SUV_2 (baseline) × 100 (%).

Statistical analysis

Each tumor was staged according to the TNM classification of the International Union Against Cancer (UICC) and the International Federation of Gynecology and Obstetrics (FIGO) Committee on Gynecologic Oncology [18, 19]. The mean follow-up period was 240 days (range 53–425 days). All variables were assessed on a patient-by-patient basis. Student's *t* test was used for paired comparisons of SUV. The McNemar test with Bonferroni's correction was used for paired comparisons between the results obtained by staging of ^{11}C-choline PET/CT. Therapeutic response was compared with imaging parameters using the Pearson correlation test. Correlation at a *P* value of less than 0.05 was considered to indicate a statistically significant difference. All data analysis was performed using software package SPSS 16.0J (SPSS, Chicago, IL, USA).

Results

Staging in cervical carcinoma

There were 11 cervical carcinomas (Table 1). Their histologic diagnoses were squamous cell carcinoma ($n = 8$), small cell carcinoma ($n = 2$), and adenosquamous carcinoma ($n = 1$). The tumor size of cervical carcinomas was 35 ± 14 mm. T stage was T1 in 2 patients (18%), T2 in 4 patients (36%), T3 in 3 patients (27%), and T4 in 1 patient (6%). The patient with T4 disease had rectal invasion microscopically. T stage was correctly classified by MRI alone in 6 patients (100%), by PET/CT alone in 3 patients (50%), and by PET/CT plus MRI in 6 patients (100%). Six (55%) of the 11 patients had N1 disease (Table 2). The accuracy of N staging was 73% by MRI alone, 91% by PET/CT alone, and 91% by PET/CT plus MRI. One patient had M1 disease with involvement of a paraaortic lymph node. The accuracy of M staging was 100% by PET/CT plus MRI as well as by PET/CT alone.

Staging in corpus carcinoma

The histologic diagnoses of 11 corpus carcinomas (Fig. 1) were endometrioid adenocarcinoma ($n = 9$), carcinosarcoma ($n = 1$), and serous adenocarcinoma ($n = 1$). The histologic grades of the corpus carcinomas were Grade 1 ($n = 6$), Grade 2 ($n = 3$), and Grade 3 ($n = 2$). No significant differences in SUV_1 ($p = 0.236$) or SUV_2 ($P = 0.348$) of the primary lesion were found between cervical carcinoma and corpus carcinoma (Fig. 1). The δSUV in each type of tumor was similar at both primary sites ($P = 0.347$). The tumor size of the corpus carcinomas was 36 ± 21 mm. T stage was T1 in 5 patients (45%), T2 in 1 patient (6%), and T3 in 5 patients (45%). T stage was correctly classified by MRI alone in 9 patients (82%), by PET/CT alone in 5 patients (45%), and by PET/CT plus MRI in 10 patients (91%). One patient with corpus carcinoma who had developed a vaginal metastasis was understaged by MRI alone. After adding interpretation of PET/CT which showed discrete uptakes in the corpus and

Table 1 Demographic data of patients with cervical and corpus carcinomas

Parameter	Cervical carcinoma	Corpus carcinoma	Total
No. of patients	11	11	22
Age			
Mean ± SD	49 ± 12	53 ± 12	51 ± 12
Range	33–68	31–73	31–73
SUV_1			
Mean ± SD	4.83 ± 1.87	5.92 ± 2.30	5.37 ± 2.12
Range	2.06–9.42	2.71–9.31	2.06–9.42
SUV_2			
Mean ± SD	4.98 ± 1.97	5.82 ± 2.10	5.40 ± 2.04
Range	2.30–10.01	3.00–9.31	2.30–10.01
δSUV (%)			
Mean ± SD	−4.05 ± 14.01	0.40 ± 6.28	−1.82 ± 10.84
Range	−39.67–14.25	−10.70–14.00	−39.67–14.25
Final stage	IB ($n = 2$)	IA ($n = 1$)	
	IIB ($n = 4$)	IB ($n = 4$)	
	IIIB ($n = 3$)	IIA ($n = 1$)	
	IVB ($n = 1$)	IIIA ($n = 2$)	
		IIIB ($n = 1$)	
		IIIC ($n = 2$)	

SD standard deviation, *SUV_1* SUV at a mean uptake time of 5 min, *SUV_2* SUV at a mean uptake time of 18 min

Table 2 Location of metastatic lymph nodes in all patients

Lymph node	No. of patients
Obturator	8 (36.3)
Common iliac	3 (13.6)
Paraaortic	2 (9.0)
External iliac	2 (9.0)
Internal iliac	2 (9.0)
Suprainguinal	1 (4.5)

The numbers in parentheses are percentages

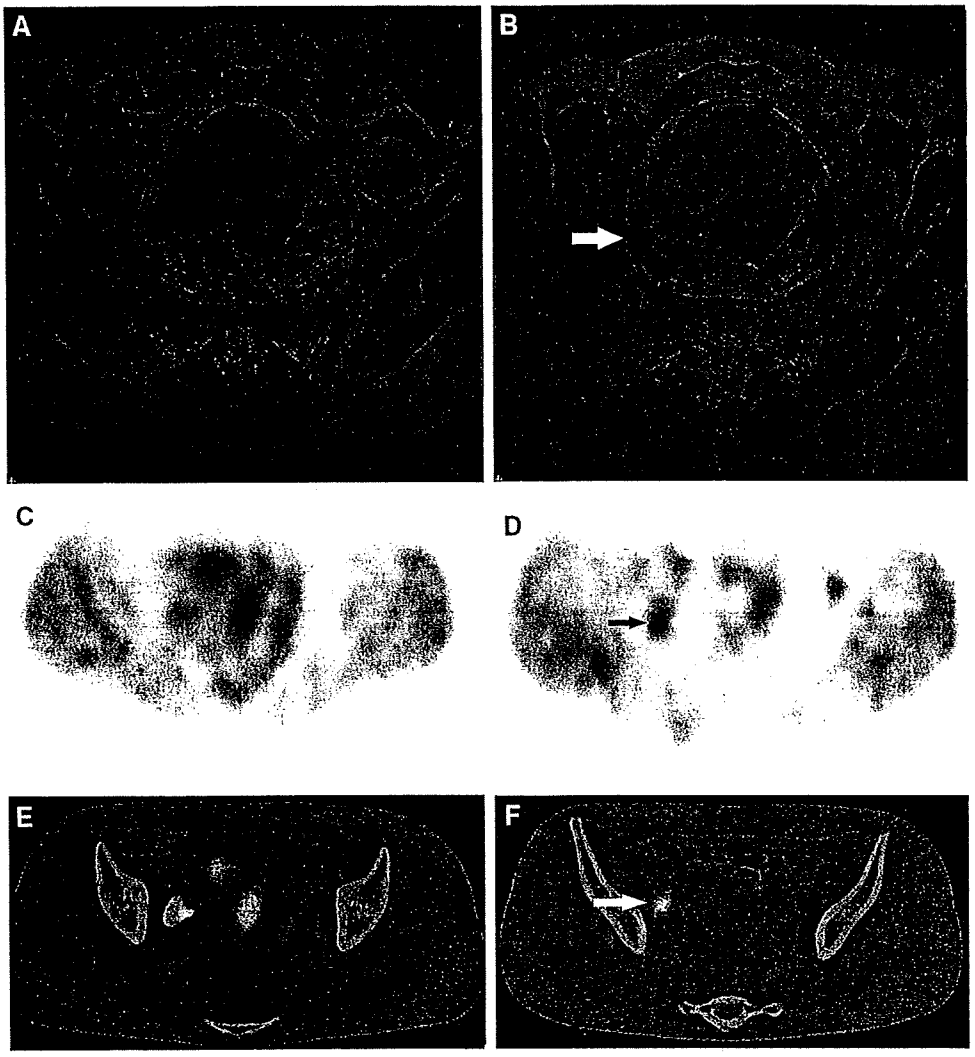

Fig. 1 A 52-year-old woman with corpus carcinoma. **a, b** Transverse T2-weighted MR image (TR/TE_{eff}: 4,000 ms/100 ms) shows a primary tumor of the isthmus and enlargement of the right obturator lymph node (*arrow*). **c, d** Transverse ^{11}C-choline PET image reveals a hypermetabolic focus in the primary tumor and right obturator region (*arrow*). **e, f** Transverse ^{11}C-choline PET/CT image reveals a hypermetabolic focus in the primary tumor and right obturator lymph node (*arrow*). PET/CT findings were verified by histopathologic analysis

vagina, this patient was correctly diagnosed as having a vaginal metastasis. A patient with corpus carcinoma and peritoneal dissemination was understaged by MRI alone, whereas staging by PET/CT alone or PET/CT plus MRI was correct. Three (27%) of the 11 patients had N1 disease. The accuracy of N staging was 64% by MRI alone, 82% by PET/CT alone, and 100% by PET/CT plus MRI. All patients had M0 disease. The accuracy of M staging was 91% by PET/CT plus MRI and 82% by PET/CT alone. PET/CT alone overstaged two patients with corpus carcinoma as having distant metastasis, and their definitive diagnosis was vaginal metastasis and normal paraaortic lymph node, respectively. One patient with corpus carcinoma was overstaged by PET/CT plus MRI as having M1 disease.

Staging performance in uterine carcinomas

T stage (Table 3) was correctly classified by MRI alone in 15 patients (88%), by PET/CT alone in 8 patients (47%), and by PET/CT plus MRI in 16 patients (94%). MRI alone or PET/CT plus MRI was superior to PET/CT alone in determining T stage ($P = 0.039$ or $P = 0.008$, respectively). PET/CT alone understaged four patients and overstaged five patients. The accuracy of N staging (Table 3) was 68% by MRI alone, 86% by PET/CT alone, and 96% by PET/CT plus MRI. PET/CT plus MRI was superior to MRI alone in assigning N stage ($P = 0.031$). MRI alone understaged four patients with subcentimetric lymph node and overstaged three patients with reactive lymph nodes. However, PET/CT alone understaged two patients with lymph node fewer than 10 mm in diameter and overstaged one patient with reactive lymph node. One patient with a lymph node was understaged by PET/CT plus MRI. The accuracy of M staging (Table 3) was 96% by PET/CT plus MRI and 91% by PET/CT alone. The overall stage (Table 3) was correctly diagnosed by PET/CT in 47%, and by PET/CT plus MRI in 88% ($P = 0.039$). PET/CT alone led to assignment of an incorrect TNM stage in nine patients due to misdiagnosis of T stage. Two patients were incorrectly diagnosed by PET/CT plus MRI.

Consequently, the misdiagnoses were in a patient with corpus carcinoma who had vaginal metastasis and a patient with a lymph node that measured fewer than 10 mm in diameter.

Table 3 Comparison of the diagnostic accuracy of staging by MRI, PET/CT, and combining PET/CT and MRI (PET/CT+MRI)

Diagnosis	MRI	PET/CT	PET/CT+MRI
T stage ($n = 17$)			
Correct	15 (88.2)*	8 (47.1)*†	16 (94.1)†
Overstaged	0	5 (29.4)	0
Understaged	2 (11.8)	4 (23.5)	1 (5.9)
N stage ($n = 22$)			
Correct	15 (68.2)†	19 (86.4)	21 (95.5)†
Overstaged	3 (13.6)	1 (4.5)	0
Understaged	4 (18.2)	2 (9.1)	1 (4.5)
M stage ($n = 22$)			
Correct	NA	20 (90.9)	21 (95.5)
Overstaged	NA	2 (9.0)	1 (4.5)
Understaged	NA	0	0
Overall stage ($n = 17$)			
Correct	NA	8 (47.1)†	15 (88.2)†
Overstaged	NA	5 (29.4)	1 (5.9)
Understaged	NA	4 (23.5)	1 (5.9)

The numbers in parentheses are percentages. The diagnostic accuracy of two modalities was compared by the McNemar test. Significant differences were found between two groups: * $P < 0.01$ and † $P < 0.05$

NA not applicable

Evaluation of therapeutic effect

Four (80%) of the five patients had IIb disease and one patient (20%) had IVa disease. One patient with IVa disease had bladder invasion and suffered from secondary bilateral hydronephrosis. Three patients (60%) had pelvic lymph node enlargement. Two of them were detected in bilateral obuturator enlarged lymph nodes, and the other in right obuturator enlarged lymph node. Distant metastases were not detected in any patients.

Baseline MRI showed that tumor size was 36.5 ± 8.7 mm. After treatment, the mean size was reduced to 21.8 ± 8.2 mm. Baseline MRI showed a tumor volume of 20.2 ± 12.6 cm^3. After treatment, the mean volume was reduced to 12.2 ± 8.4 cm^3 (Fig. 2). The %Size-RR was 40.7 ± 12.8% and the %Volume-RR was 56.5 ± 10.3% (Table 4).

All five patients had abnormal ^{11}C-choline uptake of the primary lesion on initial PET/CT. SUV_1 and SUV_2 after chemoradiotherapy decreased compared with that before chemoradiotherapy. Baseline PET/CT showed a mean SUV_1 of 5.3 ± 2.4, and a mean SUV_2 of 5.2 ± 2.7. After treatment, the SUV_1 decreased to 2.6 ± 1.2, and the SUV_2 decreased to 2.0 ± 1.0 (Fig. 2). The $\%SUV_1$-RR was 48.0 ± 20.0% and $\%SUV_2$-RR was 60.3 ± 14.4% (Table 5).

The correlation between $\%SUV_1$-RR and %Size-RR was not significant ($r = 0.698$, $P = 0.19$), while there was a significant correlation between $\%SUV_1$-RR and %Volume-RR ($r = 0.892$, $P = 0.042$). Indeed, there was

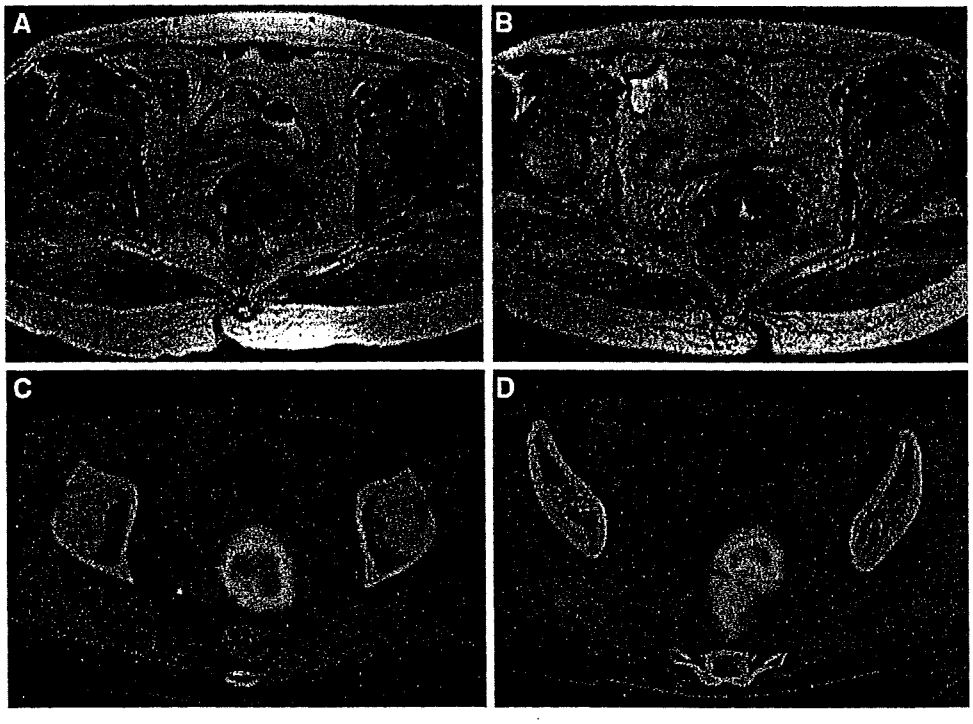

Fig. 2 A 60-year-old woman with cervical carcinoma: Transverse T2-weighted MR image on the baseline study (**a**) shows an isointense tumor of uterine cervix. The tumor size and volume are 32.6 mm and 12.59 cm^3, respectively. After treatment (**b**), the tumor is reduced in size. The tumor size and volume are 16.4 mm and 5.63 cm^3, respectively. Transverse ^{11}C-choline PET/CT image on the baseline study (**c**) shows an increased metabolic uptake in primary tumor. After treatment (**d**), metabolic uptake in the primary tumor decreases. The SUV_1 and SUV_2 decrease from 4.61 and 4.61 to 2.10 and 1.90, respectively

Table 4 Clinical characteristics in five patients with cervical carcinoma

Pt	Age	Chief complaint	Histology	Chemo		RT		Recurrence time (months)	Treatment after recurrence	Follow-up time (months)
				Dose (mg)	Cycle	EBRT	ICRT			
1	60	Vaginal bleeding	Squamous	56	1	50 Gy/25fr	18 Gy/3fr	3	Chemo	13
2	68	Vaginal bleeding	Squamous	0	0	50 Gy/25fr	18 Gy/3fr	8	None	14
3	55	Vaginal bleeding	Squamous	56	5	50 Gy/25fr	18 Gy/3fr	7	RT	16
4	35	Vaginal bleeding	Squamous	62.2	4	50 Gy/25fr	24 Gy/4fr	None	None	15
5	57	Vaginal bleeding	Squamous	63.4	4	50 Gy/25fr	18 Gy/3fr	None	None	13

Pt patient, *Chemo* chemotherapy, *RT* radiotherapy, *EBRT* extra body radiotherapy, *ICRT* intra cervical radiotherapy, *squamous* squamous cell carcinoma, *fr* fraction

Table 5 Assessment of MRI and 11C-choline PET results in five patients with cervical carcinoma

Pt	MRI							
	Diameter (mm)				Volume (cm^3)			
	Baseline	After	δ	RR (%)	Baseline	After	δ	RR (%)
1	32.6	16.4	16.2	49.7	12.59	5.63	6.96	55.3
2	40.7	28.4	12.3	30.2	31.64	14.78	16.86	53.3
3	45.5	32.7	12.8	28.1	21.37	8.57	12.81	59.9
4	23.3	14.5	8.8	37.8	2.99	1.71	1.28	42.9
5	40.6	17.1	23.5	57.9	32.27	9.27	23.01	71.3
Pt	^{11}C-choline PET							
	SUV_1				SUV_2			
	Baseline	After	δ	RR (%)	Baseline	After	δ	RR (%)
1	9.42	4.29	5.13	54.5	10.01	3.6	6.41	64
2	3.57	2.6	0.97	27.2	3.57	1.51	2.06	57.7
3	4.61	2.1	2.51	54.4	4.61	1.9	2.71	58.8
4	4.28	3.04	1.24	29	3.67	2.19	1.48	40.3
5	4.4	1.1	3.3	75	4.1	0.8	3.3	80.5

Pt patient, *Baseline* baseline study, *After* study after treatment, δ difference between baseline study and study after treatment, *RR* reduction rate

no significant correlation between %SUV_2-RR and %Size-RR ($r = 0.660$, $P = 0.226$), while there was a significant correlation between %SUV_2-RR and %Volume-RR ($r = 0.956$, $P = 0.011$). During a mean follow-up time of 14.2 ± 1.0 months, two patients developed disease recurrence. One patient had a local recurrence three months after the treatment, and received additional chemotherapy using cisplatin and paclitaxel. The other patient developed metastasis of a paraaortic lymph node seven months after the treatment, and received radiotherapy of the abdomen. No patients died before disease recurrence.

Discussion

The results of the present study show that ^{11}C-choline PET/CT contributes to accurate staging in patients with uterine carcinoma. Specifically, the combination of ^{11}C-choline PET/CT and MRI has potential implications for determining T and N stage at the preoperative evaluation. The results of the present study also indicate that ^{11}C-choline PET/CT may be feasible as a method of evaluating the therapeutic response after chemoradiotherapy in patients with cervical carcinoma.

Clinically, requirements for an acceptable method of preoperative staging of uterine carcinoma are that it allows determination of appropriate indications for surgery. Measured by this criterion, MRI has long been recognized as the most accurate modality, with high sensitivity [20, 21]. However, the limitation in MR evaluation for preoperative staging of uterine carcinoma is low specificity for N staging. In our study the interpretation of N staging by combining ^{11}C-choline PET/CT and MRI yielded an accuracy of 96%. The results of the present study suggest

that it will be feasible to diagnose preoperative nodal status in patients with uterine carcinoma. ^{11}C-choline PET/CT may complement MRI for diagnosing nodal status prior to operation in uterine carcinoma.

Physiological distribution of ^{11}C-choline uptake in vivo can affect signal-to-background ratio for imaging in malignant tumors. After intravenous administration of ^{11}C-choline, blood clearance is rapid and radioactive distribution in tissues reaches a steady state within five minutes. Normal uptake of ^{11}C-choline is observed in the liver, pancreas, kidney, duodenum, bone marrow, and secretion into phospholipid-rich pancreatic juice is also found in the non-fasting state. The physiological background level of ^{11}C-choline in the urinary tract is lower than that of 18-fluorodeoxyglucose (18F-FDG) because of incomplete tubular reabsorption of the intact tracer [22, 23] and enhanced excretion of labeled oxidative metabolites. Although we found one false-positive case for N staging by ^{11}C-choline PET/CT, this was attributable to a reactive lymph node on microscopic observation, not to ^{11}C-choline uptake in the urinary tract. Thus, accumulation of ^{11}C-choline in the pelvis is hardly affected by urinary uptake.

The limited spatial resolution and partial volume effect of PET/CT often result in failure to detect small lesions. In our study, two patients were understaged due to the presence of a metastatic lymph node fewer than 10 mm in diameter that was visualized by the CT portion of PET/CT or by MRI. Slight increases in tracer uptake and motion artifacts caused by respiration will give rise to false-negative results. On the other hand, the false-positive results were observed in one patient-by PET/CT and in three patients by MRI because of reactive lymph nodes. The advantage of the combining PET/CT and MRI was that it decreased the number of understaged and overstaged cases by correlating the morphologic and metabolic findings.

Evaluating the therapeutic response after chemoradiotherapy requires imaging modalities, such as CT or MRI that are generally standard. However, these anatomical imaging modalities have limitations, because it takes weeks or months to evaluate therapeutic response and it is difficult to distinguish residual tumor from fibrotic and necrotic tissue. Some investigators showed the efficacy of 18F-FDG-PET in monitoring therapeutic response in patients with cervical carcinoma [12–15]. Similar to the results of 18F-FDG-PET studies, all five patients had abnormal ^{11}C-choline uptake of cervical carcinoma on the baseline study, and had decreased ^{11}C-choline uptake compared with the baseline study after chemoradiotherapy in our study.

18F-FDG-PET-derived parameters including SUV and the percent change value may have the potential to predict the therapeutic response in patients with advanced gynecological cancer. Yoshida and colleagues reported that the decrease in SUV of 18F-FDG-PET was better correlated with histological response than was MRI in three patients with advanced cervical carcinoma after neoadjuvant chemotherapy. Similarly, the present study demonstrates that %SUV_1-RR and %SUV_2-RR calculated from ^{11}C-choline PET/CT correlated well with %volume-RR calculated from MRI.

Some limitations as to setup must be resolved before the results can be transposed to routine clinical settings. Our retrospective study included only a small population with uterine carcinomas which included not only cervical carcinoma but also corpus carcinoma. Moreover, the number of patients in whom the therapeutic response to chemoradiotherapy was monitored was also small. Since our study was designed to assess staging prior to surgery, the results from this patient population with uterine carcinoma will not explain the staging accuracy of advanced disease. Long term follow-up is needed as to whether therapeutic response evaluated by ^{11}C-choline PET/CT can accurately reflect prognosis or not. ^{11}C-choline seems to be a sensitive PET tracer for the management of uterine carcinoma. However, the short half-life of ^{11}C-choline is the main cause of practical restriction. ^{18}F-choline has a longer half-life than ^{11}C-choline and has been used to diagnose prostate carcinoma [24, 25]. The sensitivity values may be affected by differences in urinary secretion, because there is no other reason why these differences between ^{18}F-choline and ^{11}C-choline should lead to improved accuracy of PET/CT.

The total numbers of patients were small and heterogeneous, and our present study is retrospective and reflects our initial experience. Further studies involving a larger number of patients and histological correlation are required to determine the clinical usefulness of ^{11}C-choline PET/CT in monitoring the therapeutic response to chemoradiotherapy in patients with cervical carcinoma.

In conclusion, combining ^{11}C-choline PET/CT and MRI increases the accuracy of staging in patients with uterine carcinoma. ^{11}C-choline PET/CT may be feasible as a method of evaluating therapeutic response after chemoradiotherapy in patients with cervical carcinoma. The results demonstrated its advantages and potential in ^{11}C-choline PET/CT, but clinical evaluation in a large patient population is warranted before applying it as an optional approach for the management of uterine carcinoma.

Acknowledgments This work was supported in part by grants from Scientific Research Expenses for Health and Welfare Programs and the Grant-in-Aid for Cancer Research from the Ministry of Health, Labour and Welfare.

References

1. Hara T, Kosaka N, Shinoura N, Kondo T. PET imaging of brain tumor with [methyl-^{11}C]choline. J Nucl Med. 1997;38:842–7.

2. Hara T, Kosaka N, Kishi H. PET imaging of prostate cancer using carbon-11-choline. J Nucl Med. 1998;39:990–5.
3. Jager PL, Que TH, Vaalburg W, Prium J, Elsinga P, Plukker JT. Carbon-11 choline or FDG-PET for staging of oesophageal cancer? Eur J Nucl Med. 2001;28:1845–9.
4. Pieterman RM, Que TH, Elsinga PH, Pruim J, van Putten JW, Willemsen AT, et al. (11)C-choline and (18)F-FDG PET in primary diagnosis and staging of patients with thoracic cancer. J Nucl Med. 2002;43:167–72.
5. de Jong IJ, Prium J, Elsinga PH, Vaalburg W, Mensink HJ. Preoperative staging of pelvic lymph nodes in prostate cancer by 11C-choline PET. J Nucl Med. 2003;44:331–5.
6. Picchio M, Treiber U, Beer AJ, Metz S, Bossner P, van Randenborgh H, et al. Value of 11C-choline PET and contrast-enhanced CT for staging of bladder cancer: correlation with histopathologic findings. J Nucl Med. 2006;47:938–44.
7. Tian M, Zhang H, Oriuchi N, Higuchi T, Endo K. Comparison of ^{11}C-choline PET and FDG PET for the differential diagnosis of malignant tumors. Eur J Nucl Med Mol Imaging. 2004;31:1064–72.
8. Scher B, Seitz M, Albinger W, Tiling R, Scherr M, Becker HC, et al. Value of (11)C-choline PET and PET/CT in patients with suspected prostate cancer. Eur J Nucl Med Mol Imaging. 2007;34:45–53.
9. Torizuka T, Kanno T, Futatsubashi M, Okada H, Yoshikawa E, Nakamura F, et al. Imaging of gynecologic tumors: comparison of ^{11}C-choline PET with ^{18}F-FDG PET. J Nucl Med. 2003; 44:1051–6.
10. Therasse P, Arbuck SG, Eisenhauer EA, Wanders J, Kaplan RS, Rubinstein L, et al. New guidelines to evaluate the response to treatment in solid tumors. European Organization for Research and Treatment of Cancer, National Cancer Institute of the United States, National Cancer Institute of Canada. J Natl Cancer Inst. 2000;92:205–16.
11. Young H, Baum R, Cremerius U, Herholz K, Hoekstra O, Lammertsma AA, et al. Measurement of clinical and subclinical tumour response using [18F]-fluorodeoxyglucose and positron emission tomography: review and 1999 EORTC recommendations. European Organization for Research and Treatment of Cancer (EORTC) PET Study Group. Eur J Cancer. 1999;35: 1773–82.
12. Nakamoto Y, Eisbruch A, Achtyes ED, Sugawara Y, Reynolds KR, Johnston CM, et al. Prognostic value of positron emission tomography using F-18-fluorodeoxyglucose in patients with cervical cancer undergoing radiotherapy. Gynecol Oncol. 2002; 84:289–95.
13. Grigsby PW, Siegel BA, Dehdashti F, Rader J, Zoberi I. Post-therapy [18F] fluorodeoxyglucose positron emission tomography in carcinoma of the cervix: response and outcome. J Clin Oncol. 2004;22:2167–71.
14. Yoshida Y, Kurokawa T, Kawahara K, Yagihara A, Tsuchida T, Okazawa H, et al. Metabolic monitoring of advanced uterine cervical cancer neoadjuvant chemotherapy by using [F-18]-Fluorodeoxyglucose positron emission tómography: preliminary results in three patients. Gynecol Oncol. 2004;95:597–602.
15. Xue F, Lin LL, Dehdashti F, Miller TR, Siegel BA, Grigsby PW. F-18 fluorodeoxyglucose uptake in primary cervical cancer as an indicator of prognosis after radiation therapy. Gynecol Oncol. 2006;101:147–51.
16. Bar-Shalom R, Yefremov N, Guralnik L, Gaitini D, Frenkel A, Kuten A, et al. Clinical performance of PET/CT in evaluation of cancer: additional value for diagnostic imaging and patient management. J Nucl Med. 2003;44:1200–9.
17. Hara T, Yuasa M. Automated synthesis of [^{11}C]choline, a positron-emitting tracer for tumor imaging. Appl Radiat Isot. 1999; 50:531–3.
18. Sobin LH, Wittekind C. UICC TNM classification of malignant tumours. 6th ed. New York: Wiley; 2002.
19. Benedet JL, Bender H, Jones H III, Ngan HY, Pecorelli S. FIGO staging classifications and clinical practice guidelines in the management of gynecologic cancers. FIGO Committee on Gynecologic Oncology. Int J Gynaecol Obstet. 2000;70:209–62.
20. Togashi K, Nishimura K, Sagoh T, Minami S, Noma S, Fujisawa I, et al. Carcinoma of the cervix: staging with MR imaging. Radiology. 1989;171:245–51.
21. Manfredi R, Mirk P, Maresca G, Margariti PA, Testa A, Zannoni GF, et al. Local-regional staging of endometrial carcinoma: role of MR imaging in surgical planning. Radiology. 2004;231:372–8.
22. Grigsby PW, Siegel BA, Dehdashti F. Lymph node staging by positron emission tomography in patients with carcinoma of the cervix. J Clin Oncol. 2001;19:3745–9.
23. Sironi S, Buda A, Picchio M, Perego P, Moreni R, Pelleqrino A, et al. Lymph node metastasis in patients with clinical early-stage cervical cancer: detection with integrated FDG PET/CT. Radiology. 2006;238:272–9.
24. Heinisch M, Dirisamer A, Loidl W, Stoiber F, Gruy B, Haim S, et al. Positron emission tomography/computed tomography with F-18-fluorocholine for restaging of prostate cancer patients: meaningful at PSA <5 ng/ml? Mol Imaging Biol. 2006;8:43–8.
25. Gutman F, Aflalo-Hazan V, Kerrou K, Montravers F, Grahek D, Talbot JN. 18F-choline PET/CT for initial staging of advanced prostate cancer. AJR Am J Roentogenol. 2006;187:618–21.

Surg Today (2009) 39:144–147
DOI 10.1007/s00595-008-3811-x

SURGERY TODAY

Middle-Colic Artery Aneurysm Associated with Segmental Arterial Mediolysis, Successfully Managed by Transcatheter Arterial Embolization: Report of a Case

TAKAHISA HIROKAWA[1,3], HIROZUMI SAWAI[1], KOJI YAMADA[1], TAKEHIRO WAKASUGI[1], HIROMITSU TAKEYAMA[1], HIROYUKI OGINO[2], MASAKATSU TSURUSAKI[3], and YASUAKI ARAI[3]

Departments of [1]Gastroenterological Surgery and [2]Radiology, Nagoya City University Graduate School of Medical Sciences, Nagoya, Japan
[3]Department of Diagnostic Radiology, National Cancer Center Hospital, 5-1-1 Tsukiji, Chuo-ku, Tokyo 104-0045, Japan

Abstract
An aneurysm of the middle-colic artery, associated with segmental arterial mediolysis (SAM), is a rare condition. This report describes a case of a middle-colic artery aneurysm that was associated with SAM. A 57-year-old man was admitted to our hospital because of severe abdominal pain. A rupture of a middle-colic artery aneurysm was diagnosed by computed tomography, and angiography showed that it may have been associated with SAM. The ruptured aneurysm was successfully treated with transcatheter arterial embolization. Transcatheter arterial embolization might be one of the best treatments for such a complicated aneurysm occurring in a visceral artery.

Key words Middle-colic artery aneurysm · Segmental arterial mediolysis · Transcatheter arterial embolization

Introduction

The most frequent site of a visceral artery aneurysm is the splenic artery, but it is a rare occurrence. Therefore, an aneurysm of the middle-colic artery is even more uncommon.[1] An aneurysm that may be caused by segmental arterial mediolysis (SAM) is also a rare condition. This report documents a case of a SAM-associated, ruptured, middle-colic artery aneurysm that was successfully managed by transcatheter arterial embolization (TAE).

Reprint requests to: T. Hirokawa (address 3)
Received: February 25, 2008 / Accepted: May 14, 2008

Case Report

A 57-year-old man with no previous medical history was admitted to a local hospital because of severe abdominal pain and diarrhea. Contrast-enhanced computed tomography (CT) showed ascites throughout the abdomen and higher CT-value ascites rather than serous ascites in the upper abdomen. Abdominocentesis revealed the presence of hemoperitoneum. Angiography located the aneurysm within the left branch of middle-colic artery, but no extravagation was seen. The CT scan revealed a hematoma around the transverse mesocolon (Fig. 1) indicating a rupture of this aneurysm. Therefore the patient was transferred to this hospital. When he arrived, his vital signs included a low grade fever (37.5°C), hypertension (184/86 mmHg), and a slight tachycardia (102 beats/min). He was not pale and had clear consciousness. A physical examination revealed only slight abdominal tenderness. The laboratory findings showed anemia (red blood cell count: 2.5 million/μl; hemoglobin: 8.4 g/dl; hematocrit: 24.3%) and inflammation (white blood cell count: 7200/μl, C-reactive protein: 4.58 mg/dl).

Angiography detected a middle-colic artery aneurysm, a wide and narrow irregularity in the distal artery of the aneurysm, but no extravagation (Fig. 2a). The results also indicated that this aneurysm was ruptured and it had a risk of further bleeding. Transcatheter arterial embolization was applied initially because it was less invasive treatment than surgery. Using a right femoral artery approach, a 4-Fr C2 catheter (Clinical Supply, Hashima, Japan) was placed in the superior mesenteric artery, and the proximal middle-colic artery was selected with micro-catheter (Renegade; Boston Scientific Japan, Tokyo, Japan). However, because of the meandering of the middle-colic artery, the microcatheter could not be inserted at the aneurysm. Therefore, microcoils could not be used. Then approximately 0.3 ml of iodized oil (Lipiodol) mixed with *N*-butyl-2-

cyanoacrylate (NBCA) (Lipiodol:NBCA = 3:2) was injected into the root of the distal branch via the aneurysm. Postembolization angiography demonstrated no filling of the aneurysm. On delayed images, the distal arteries of the aneurysm were barely evident, thus the risk of ischemic colitis was low (Fig. 2b), and surgical treatment was avoided. In addition, further arterial examinations were conducted. Celiac angiography revealed two other aneurysms. One was at the root of the celiac artery and the other at the left hepatic artery. Inferior mesenteric arterial angiography found no aneurysm, but a wide and narrow irregularity was seen. These observations suggested that these abnormal angiographic findings and aneurysms might therefore be related to SAM.

The patient's post-TAE course was uneventful and his anemia improved. A contrast-enhanced CT scan obtained 2 days later showed that the size of the hematoma had decreased and the aneurysm had been embolized (Fig. 3). The patient was discharged 1 week after TAE. Colonoscopy 3 months later showed no evidence of bowel ischemia, and he is currently doing well without symptoms.

Discussion

Visceral aneurysms are relatively rare. The most common sites of visceral arterial aneurysms are the splenic artery (60%), hepatic artery (20%), superior mesenteric artery (5.5%), celiac artery, gastric and gastroepiploic arteries (4%), and jejunal, ileal, and colonic arteries and their tributaries (3%).[1] Aneurysms of the superior mesenteric arterial branch, particularly the middle-colic artery, are very uncommon. These are generally asymptomatic and are usually found incidentally.

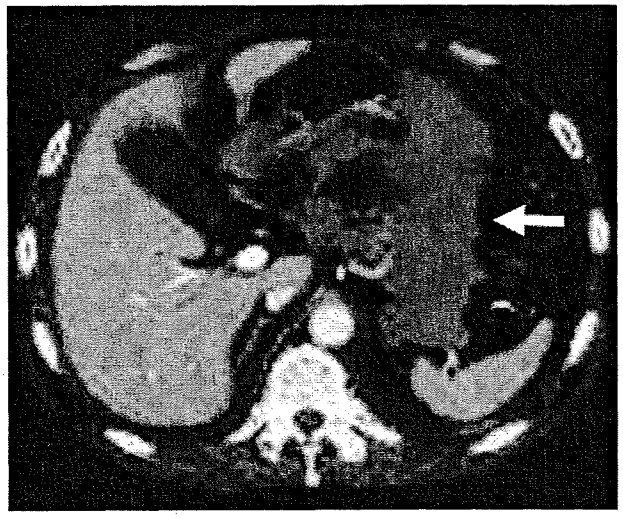

Fig. 1. Contrast-enhanced computed tomography (CT) scan shows extensive ascites in the omental bursa and around the transverse mesocolon (*arrow*)

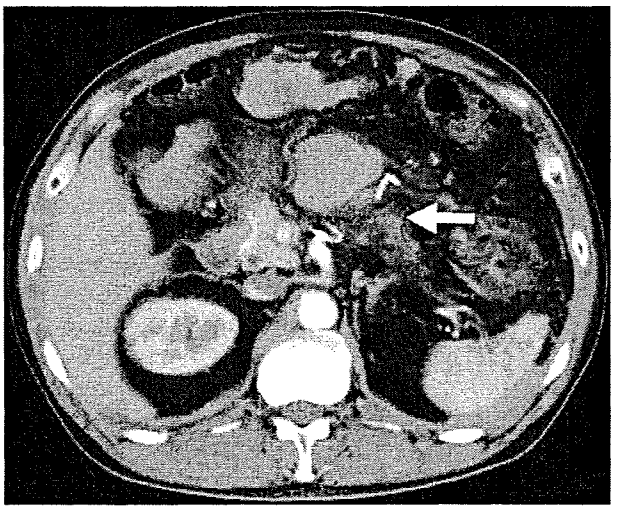

Fig. 3. The successful embolization of the aneurysm of the middle-colic artery is shown on contrast-enhanced CT scan at 2 days after TAE (*arrow*)

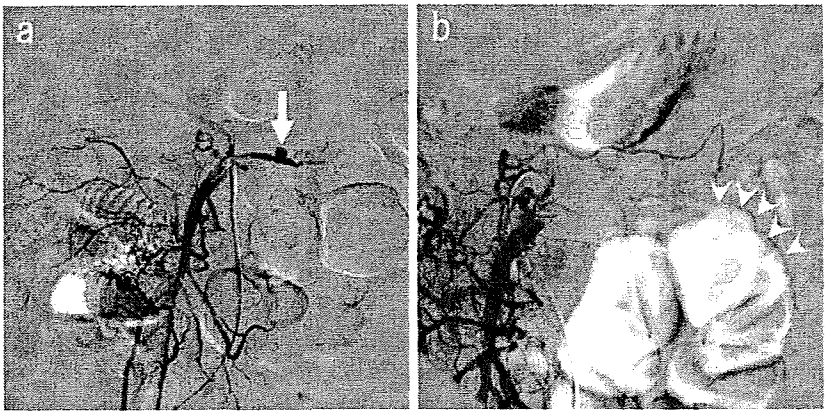

Fig. 2. a Angiography of the superior mesenteric artery shows that the aneurysm is in the left branch of middle-colic artery (*arrow*), but no extravasations are seen. **b** The left branch of the middle-colic artery was successfully embolized by transcatheter arterial embolization (TAE); there is no filling of the aneurysm. On delayed images, the distal arteries of the aneurysm are barely evident, indicating that the risk of ischemic colitis was low (*arrowheads*)

Table 1. Cases of middle colic artery aneurysms (7 cases after Sarcina et al.[2] reviewed in 2000)

First author[Ref.]	Year	Age (years)	Sex	Chief symptoms	Past history/ present illness	Diagnosis	Treatment	Other aneurysms
LaBerge[3]	1999	52	M	Abdominal pain, nausea, vomiting	Hypertension	Angiography	Resection	Yes
Sarcina[2]	2000	72	F	Dyspepsia, epigastric discomfort	Hypertension	Angiography	Resection	No
Matsuo[4]	2001	68	M	Anemia	Not described	Angiography	Resection	Not described
Sato[5]	2001	68	M	Abdominal pain	None	Surgery	Resection	No
Toyonaga[6]	2002	73	M	Abdominal pain, vomiting	Acute pancreatitis	Angiography	Embolization	No
Chino[7]	2004	78	M	Abdominal pain, nausea	Renal stones, gout	Surgery	Bowel-resection	No
Present case		57	M	Abdominal pain	None	Angiography	Embolization	Yes

Sarcina et al.[2] reviewed the literature of the 28 cases of middle-colic artery aneurysms reported between 1937 and 1995, and Medline was searched using the keywords "Middle-colic artery" and "aneurysm," and another 5 cases of middle-colic artery aneurysm were found (Table 1).[2-7] The data from the 35 reported cases, including the current case, were analyzed. The mean age and age range were 59.3 ± 13.3 years and 19–78 years, respectively. The ratio of males to females was 19:16; thus, there appears to be no significant gender difference. In almost all cases, the chief complaint was abdominal pain. In total, 45.7% of the cases (16/35) had multiple aneurysms. Most cases were treated surgically. An aneurysm ligation was performed in 11 cases, resection was performed in 8 cases, and a bowel resection was required in 9 cases. Transcatheter arterial embolization was chosen in only 3 cases. Embolization was performed using particles of gelatin sponge inserted in one case,[8] using microcoils in one case,[6] and in the present case, a mixed emulsion of Lipiodol and NBCA was used. Using this embolic agent, it was possible to embolize the aneurysm root and its proximal and distal feeders in one step. However, this procedure is associated with risks including bowel ischemia, and aneurysm rupture using this agent for the treatment of lower bowel hemorrhage or aneurysm is still controversial. Most mesenteric artery embolizations are performed using microcoils.[9] But in the present case, NBCA was used with Lipiodol because distal catheterization of the aneurysm could not be achieved. NBCA is a liquid embolic agent whose time to coagulation after injection can be controlled by diluting it with Lipiodol. It might be possible to embolize an aneurysm, feeding vessels, and efferent vessels using an NBCA–Lipiodol mixture of an appropriate concentration, even if the catheter cannot reach the aneurysm. The aneurysm in the present case was successfully embolized using this method.

Tulsyan et al.[10] studied 90 cases of visceral artery aneurysms and pseudoaneurysms and found that endovascular treatment was technically successful in 98% of the cases. In the review of 9 cases of visceral artery aneurysm by Kasirajan et al.,[11] aneurysm exclusion was achieved in 75% cases by coil embolization. They concluded that percutaneous transcatheter coil embolotherapy is an effective alternative to open surgery and that therapy may decrease the morbidity and mortality associated with open surgical procedures. There have been very few reported cases of NBCA embolization for visceral artery, but there are no reports of complications including ischemia.[12] This report suggested the embolization with NBCA is a safe method. Above all, because this endovascular method is at least as safe as open surgery and less invasive, it is one of the best treatments for a visceral artery aneurysm.

The association of the aneurysms in this case to SAM was indicated by the presence of multiple aneurysms and luminal irregularities of the artery walls. The pathogenesis of SAM is poorly understood and was first described by Slavin and Gonzalez-Vitale in 1976, and at first the name "segmental mediolytic arteritis (SMA)" was coined.[13] They described unique vascular lesions, so-called mediolytic lesions, in three autopsy cases of SMA, which were characterized by lytic degeneration of the arterial media. Based on their later observations, together with the inconstant association of inflammation in the involved arteries and the general absence of clinical and laboratory evidence of vasculitis, the term SMA was changed to "segmental arterial mediolysis (SAM)" in 1995.[14] From this etiology, this disease is also called "segmental mediolytic arteriopathy," but now the name "SAM" is the most frequently used. According to a review of 20 cases of SAM involving abdominal splanchnic arteries by Takagi et al.,[15] SMA occurs in middle-aged to elderly people (range, 39–87 years) of

both sexes, usually involves more than one visceral artery, and most frequently, branches of the celiac axis. The current case was compatible with these cases. Generally the visceral aneurysms are related to an infection represented by subacute bacterial endocarditis, polyarteritis nodosa, and others. In the present case, there had been no previous infectious disease. Following the TAE, the patient is doing well and there have been no signs of inflammation, and thus no need for any steroid or immunosuppressive drug therapies. One limitation to this study is that no pathological examination was carried out, but the clinical and radiographical findings strongly suggested SAM. In conclusion, this was a rare case of a ruptured middle-colic artery aneurysm associated with SMA, which is the first case to be treated by Lipiodol and NBCA embolization.

References

1. Moore WS. Vascular surgery: a comprehensive review. 3rd ed. Philadelphia, PA: Saunders; 1991.
2. Sarcina A, Bellosta R, Magnaldi S, Luzzani L. Aneurysm of the middle colic artery — case report and literature review. Eur J Vasc Endovasc Surg 2000;20:198–200.
3. LaBerge K. SCVIR Annual Meeting film panel session: case 3. JVIR 1999;10:509–13.
4. Matsuo S, Yamaguchi S, Miyamoto S, Ishii T, Tsuneoka N, Obata S, et al. Ruptured aneurysm of the visceral artery: report of two cases. Surg Today 2001. 31:660–4.
5. Sato T, Itoh M, Ohta N, Funaki H, Saito Z, Takayanagi N. Spontaneous ruptured middle colic artery aneurysm with concurrent renal cell carcinoma. Hepato-Gastroenterology 2001;48: 678–80.
6. Toyonaga T, Nagaoka S, Ouchida K, Nagata M, Shirota T, Ogawa T, et al. Case of a bleeding pseudoaneurysm of the middle colic artery complicating acute pancreatitis. Hepato-Gastroenterology 2002;49:1141–3.
7. Chino O, Kijima H, Shivuya M, Yamamoto S, Kashiwagi H, Kondo Y, et al. A case report: spontaneous rupture of dissecting aneurysm of the middle colic artery. Tokai J Exp Clin Med 2004;29:155–8.
8. Naito A, Toyota N, Ito K. Embolization of a ruptured middle colic artery aneurysm. Cardiovasc Intervent Radiol 1995;18: 56–8.
9. d'Othee BJ, Surapaneni P, Rabkin D, Nasser I, Clouse M. Microcoil embolization for acute lower gastrointestinal bleeding. Cardiovasc Intervent Radiol 2006;29:49–58.
10. Tulsyan N, Kashyap VS, Greenberg RK, Sarac TP, Clair DG, Pierce G, et al. The endovascular management of visceral artery aneurysms and pseudoaneurysms. J Vasc Surg 2006;45:276–83.
11. Kasirajan K, Greenberg RK, Clair D, Ouriel K. Endovascular management of visceral artery aneurysm. J Endovasc Ther 2001;8:150–5.
12. Kish JW, Katz MD, Marx MV, Harrell DS, Hanks SE. N-butyl cyanoacrylate embolization for control of acute arterial hemorrhage. J Vasc Interv Radiol 2004;15:689–95.
13. Slavin RE, Gonzalez-Vitale JC. Segmental mediolytic arteritis. A clinical pathologic study. Lab Interv 1976;35:23–9.
14. Slavin RE, Saeki K, Bhagavan B, Maas AE. Segmental arterial mediolysis: a precursor to fibromuscular dysplasia?. Mod Pathol 1995;8:287–94.
15. Takagi C, Ashizawa N, Eishi K, Ashizawa K, Hayashi T, Tanaka K, et al. Segmental mediolytic arteriopathy involving celiac to splenic and left renal arteries. Intern Med 2003;42:818–23.